Compound Synthesis and Characterization

All commercially available chemicals were of analytical grade and used without further purification. Preparative HPLC was performed with the system LaPrep P110 (VWR) supplied with a variable UV detector (P314, VWR) and a NUCLEODUR® Sphinx RP column (VP250/21, 5 µm 250 x 21 mm; Macherey-Nagel). The system Agilent 1100 series (Agilent Technologies) was used for semipreparative and analytical HPLC runs thereby analyzing the compounds with reversed-phase high performance liquid chromatography (RP-HPLC; Chromolith RP-18e, 100×10mm/Chromolith RP-18e, 100×4.6 mm; Merck). For semipreparative HPLC runs a linear gradient (0.1% aqueous TFA (A) to 100% B (0.1% TFA in CH_3CN)) in 10 min at 5 mL/min and for analytical HPLC runs a linear gradient (0.1% aqueous TFA (A) to 100% B (0.1% TFA in CH_3CN)) in 10 min at 2 mL/min were selected. UV absorbance was measured at 214 and 254 nm, respectively. For all final products, the chemical purity was greater than 98%, as determined by HPLC. Analytical reversed-phase HPLC of the ^{68}Ga-labeled compound Glu-urea-Lys-$(HE)_3$-HBED-CC-IRDye800CW was performed using a EC 250/4.6 NUCLEOSIL 120-5 C 18 column (Machery-Nagel) with a linear gradient 85% 0.1% aqueous TFA (A) to 60% B (0.1% TFA in CH3CN)) in 13 min at 1.5 mL/min or a Chromolith RP-18e 100x4.6 mm column with a linear gradient (0.1% aqueous TFA (A) to 100% B (0.1 % TFA in CH3CN)) in 5 min at 4 mL/min. For mass spectrometry a MALDI-MS (Daltonics Microflex, Bruker Daltonics) and 2,5-dihydroxybenzoic acid as a matrix were used.

Synthesis of Glu-urea-Lys-$(HE)_1$-HBED-CC-IRDye800CW, Glu-urea-Lys-$(HE)_3$-HBED-CC-IRDye800CW and Glu-urea-Lys-$(WE)_1$-HBED-CC-IRDye800CW

Synthesis of Glu-urea-Lys-$(HE)_1$-$CO(CH_2)_4$-N_3, Glu-urea-Lys-$(WE)_1$-$CO(CH_2)_4$-N_3 and Glu-urea-Lys-$(HE)_3$-$CO(CH_2)_4$-N_3

The pharmacophore Glu-urea-Lys was synthesized as described previously (*1*). Briefly, the isocyanate of the glutamyl moiety was formed using triphosgene in a first step. Resin-immobilized (2-chloro-tritylresin) and ε-allyloxycarbonyl protected lysin was added, the reaction stirred for 16 h at room temperature and the resin was finally filtered off. By reacting twice with $Pd(PPh_3)_4$ (0.3 eq.) and morpholine (15 eq.) in dichloromethane under ambient conditions (1 h, RT, protected from light) the allyloxy-protecting group was cleaved. To build up the different linkers the resin was split and further continued with standard Fmoc solid phase protocols. Depending on the linker sequence the coupling of the amino acids Fmoc-L-His(Trt)-OH, Fmoc-L-Glu(O*t*-Bu)-OH or Fmoc-L-Trp(Boc)-OH, 4 eq. respectively, and as a final building block 5-azidopentanoic acid (4 eq.) was performed using HBTU (4 eq.) and DIPEA (4 eq.) in DMF.

Cleavage of the products from the resin was performed for 3 hours at RT using TFA/TIPS/H_2O (95/2.5/2.5, v/v/v) resulting in the azido-functionalized intermediates, which were purified using RP-HPLC and identified via mass spectrometry.

Synthesis of Glu-urea-Lys-$(HE)_1$-HBED-CC-PEG_2, Glu-urea-Lys-$(WE)_1$-HBED-CC-PEG_2 and Glu-urea-Lys-$(HE)_3$-HBED-CC-PEG_2

As described previously, HBED-CC$(TFP)_2$ was synthesized under Fe^{3+} protection and via the formation of $[Fe(HBED\text{-}CC)]^-$ (*2*). After isolating the bis-TFP ester with preparative HPLC, [Fe (HBED-CC)]TFP_2 and 0.95 eq. of propargylamine were dissolved in DMF in the presence of DIPEA (Supplemental Figure 1). An excess of 2,2′-(ethylenedioxy)bis(ethylamine) (100 µL) was added after 4 h at RT and the resulting mixture gently stirred for 16 h at RT. The alkenyl-functionalized chelator was finally purified using preparative HPLC. Afterwards, PEG_2-

[Fe(HBED-CC-propargylamine)] (1 eq.) was reacted with the azido-functionalized intermediates of the previous step (1 eq., respectively) via CuAAC, $CuSO_4$ (1 eq.), Na-ascorbate (1 eq.), in 3 mL THF/H_2O (1:1, v/v) for 16 h at RT. The Fe-protected products were purified by preparative HPLC and identified with mass spectrometry.

Conjugation of IRDye800CW

IRDye800CW-NHS ester (1 eq.) was conjugated to Glu-urea-Lys-$(HE)_1$-[Fe(HBED-CC-PEG_2-NH_2)], Glu-urea-Lys-$(WE)_1$-[Fe(HBED-CC-PEG_2-NH_2)] and Glu-urea-Lys-$(HE)_3$-[Fe(HBED-CC-PEG_2-NH_2)], respectively, in PBS-buffer (pH 8.5) for 24 h at RT. The Fe-protected products were isolated via semipreparative HPLC and identified with mass spectrometry. Complexed Fe^{3+} was removed as described previously (*2*). Briefly, the Fe-containing products were trapped on a C18 cartridge. Subsequently, the cartridge was flushed with 10 mL 1 M HCl and washed with 5 mL H_2O. The final products were eluted with 2 mL H_2O/CH_3CN (3:1) and evaporated to dryness.

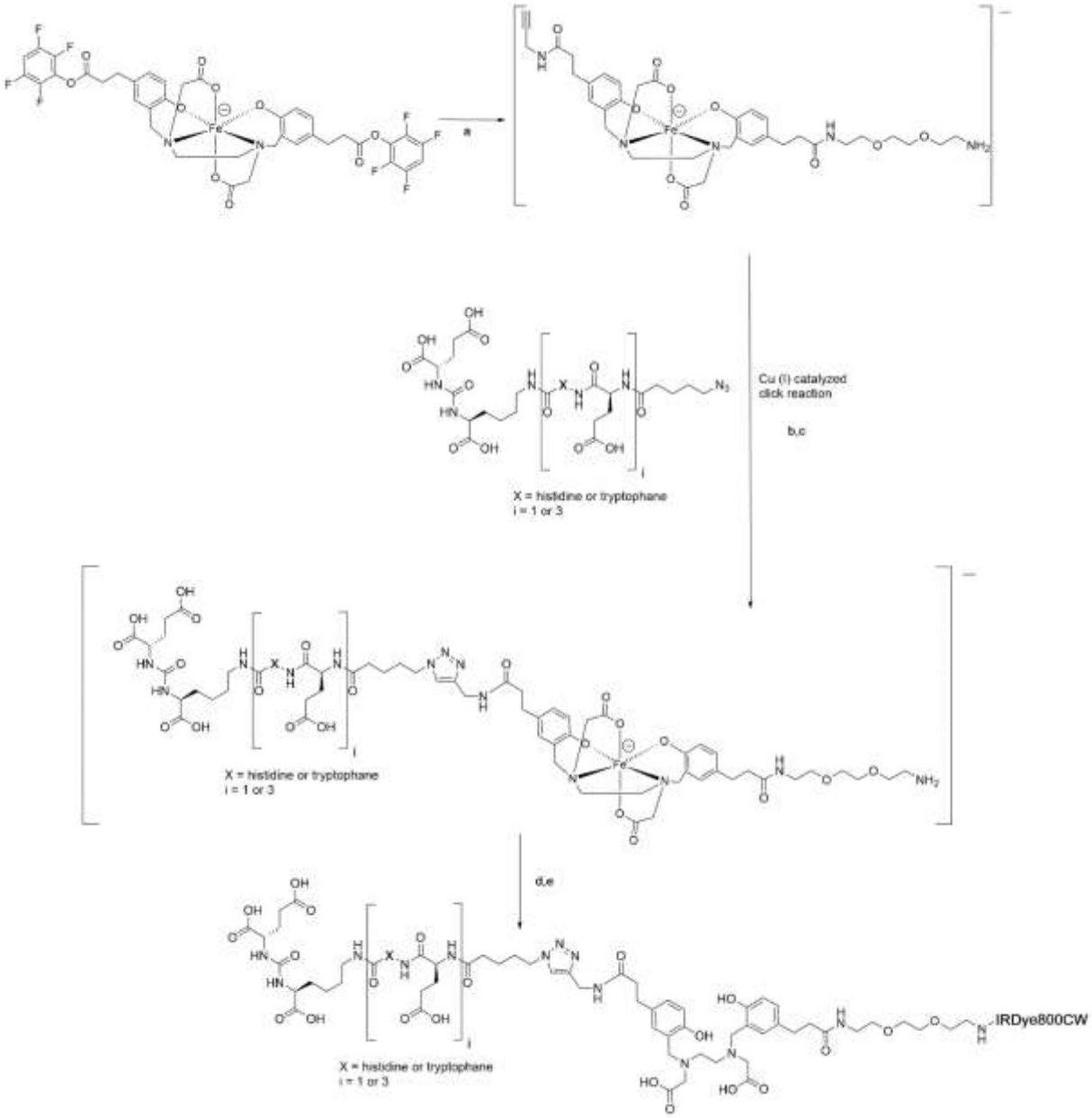

Supplemental Figure 1. Synthesis of Glu-urea-Lys-(HE)$_1$-HBED-CC-IRDye800CW, Glu-urea-Lys-(HE)$_3$-HBED-CC-IRDye800CW and Glu-urea-Lys-(WE)$_1$-HBED-CC-IRDye800CW. (a) 0.95 eq. 2-propynylamine, DIPEA, 4 h, RT; excess (100 µL) 2,2′-(ethylendioxy)bis(ethylamine), 16 h, RT, (b) 1 eq. CuSO4, (c) 1 eq. Na-ascorbate in THF/H_2O (1:1, v/v), RT, 16 h, (d) PBS-buffer (pH 8.5), 1 eq. IRDye800CW-NHS ester RT, 16 h, (e) 1 M HCl.

Synthesis of Glu-urea-Lys-HBED-CC-$(HE)_3$-IRDye800CW

In a first step PEG_2-$(EH)_3$-$CO(CH_2)_4$-N_3 was synthesized starting from an O-Bis(aminoethyl)ethylene glycol trityl resin. Based on a standard Fmoc solid phase protocol, Fmoc-L-Glu(O*t*-Bu)-OH and Fmoc-L-His(Trt)-OH (4 eq. each) were activated with HBTU (4 eq.) and DIPEA (4 eq.) and coupled in DMF. The couplings were repeated three times to obtain the $(HE)_3$-motif. Finally, 5-azidopentanoic acid (4 eq.) was coupled using HBTU (4 eq.) and DIPEA (4 eq.) in DMF. The azido-functionalized intermediate was cleaved from the resin for 3 hours at RT using TFA/TIPS/H_2O (95/2.5/2.5, v/v/v), the product purified with preparative HPLC and identified with mass spectrometry.

Subsequently, bis-TFP activated $[Fe(HBED\text{-}CC)]^-$ (**1**) was reacted with tris(*t*-Bu)-protected Glu-urea-Lys (ABX; 0.9 eq.) in DMF at RT (Supplemental Figure 2). After 4 h, 50 µL 2-propynylamine was added and the mixture stirred for 16 h at RT. The resulting Glu-urea-Lys([Fe(HBED-CC-propargylamin)]) was isolated via preparative HPLC (**2**). PEG_2-$(EH)_3$-$CO(CH_2)_4$-N_3 (1 eq.) and tris(*t*-Bu)-protected Glu-urea-Lys([Fe(HBED-CC-propargylamine)]) (1 eq.) were reacted via CuAAC, $CuSO_4$ (1 eq.), Na-ascorbate (1 eq.), in 3 mL THF/H_2O (1:1, v/v) for 16 h at RT. The tris(*t*-Bu)- and Fe-protected intermediate was separated by preparative HPLC and the tris(*t*-Bu)-protecting groups removed after lyophilisation with 3 mL TFA for 4 h at RT (**3**). In the final step IRDye800CW-NHS ester was conjugated to Glu-urea-Lys([Fe(HBED-CC-$(HE)_3$-PEG_2-NH_2)]) and complexed Fe^{3+} removed as described in the previous section (**4**).

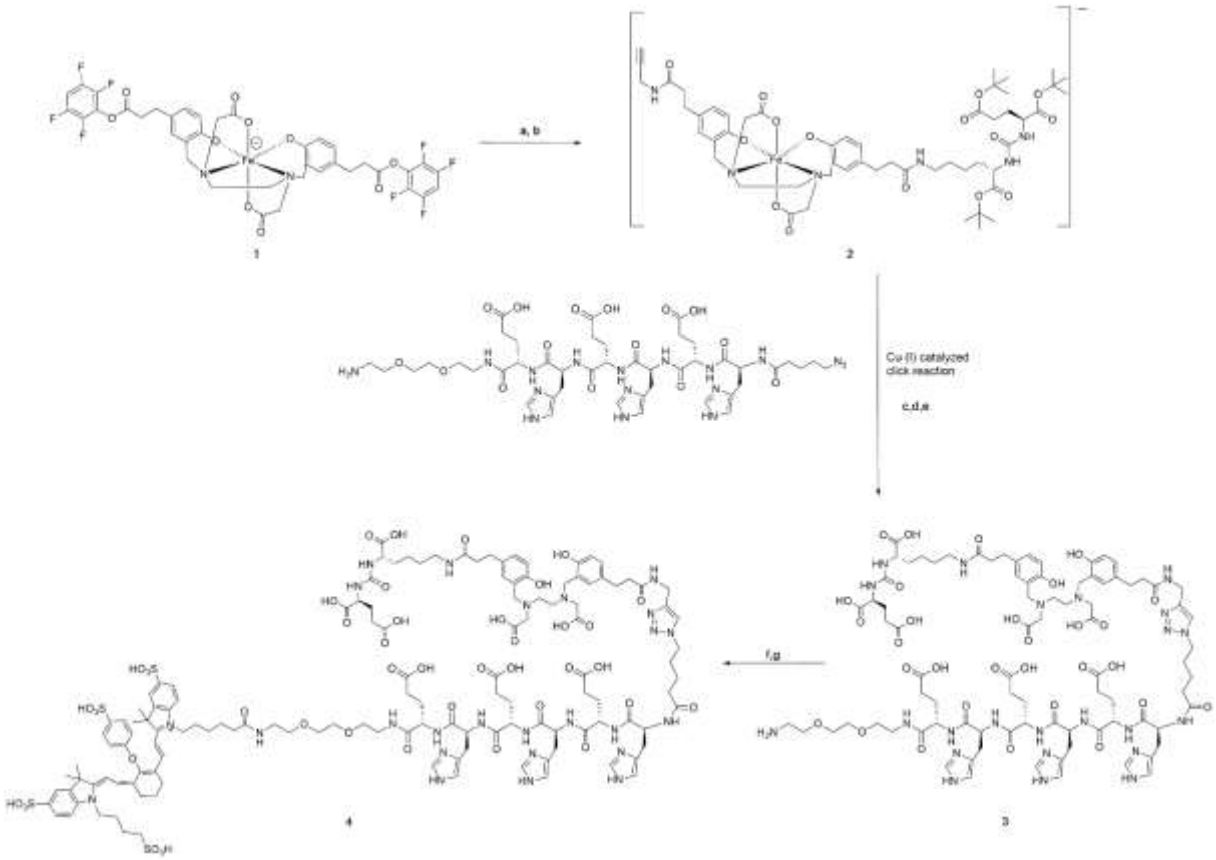

Supplemental Figure 2. Synthesis of Glu-urea-Lys-HBED-CC-(HE)$_3$-IRDye800CW. (a) 0.9 eq. tris(*t*-Bu)-protected Glu-urea-Lys in DMF, DIPEA, 4 h, RT (b) excess (50 µL) 2-propynylamine, 16 h, RT, (c) 1 eq. CuSO4, d) 1 eq. Na-ascorbate in THF/H_2O (1:1, v/v), RT, 16 h, (e) TFA, 3 h, RT, (f) PBS-buffer (pH 8.5), 1 eq. IRDye800CW-NHS ester RT, 16 h, (g) 1 M HCl.

Radiolabeling with ^{68}Ga and Determination of Lipophilicity

The precursor peptides [1 nmol in 2-[4-(2-hydroxyethyl)piperazin-1-yl]ethanesulfonic acid (HEPES) buffer (580 mg/ml) with 5 mg ascorbic acid, 90 µL] were added to 40 µL $^{68}Ga^{3+}$ eluate (~80-120 MBq). The pH was adjusted to 3.8 using 30% NaOH and 10% NaOH, respectively. The reaction mixture was incubated at 98°C for 10 minutes. The respective radiochemical yield was determined by reversed-phase high performance liquid chromatography (RP-HPLC) or reversed-phase thin layer chromatography (RP-TLC, 60 RP-18 F_{254S}) with 0.1 M sodium citrate [$HOC(COONa)(CH_2COONa)_2 \cdot 2H_2O$] as mobile phase. The 2-phase system n-octanol and PBS was used for the determination of lipophilicity of the ^{68}Ga-labeled compounds.

In Vitro Serum Stability

^{68}Ga-labeled Glu-urea-Lys-$(HE)_3$-HBED-CC-IRDye800CW (10 µL) was incubated in 100 µL human or mouse plasma (100 µL) at 37 °C. At different time points of incubation (t= 1 h, 2 h), aliquots of 10 µL were taken and plasma proteins precipitated in 30 µL acetonitrile. Samples were centrifuged for 5 min at 13000 rpm and the supernatants analysed by analytical RP-HPLC.

Preclinical Proof-of-Concept Study (PET and Optical Imaging)

The PET imaging study was performed with an Inveon µ-PET scanner (Siemens) with a dynamic scan for 60 min and a static scan (10 min) at 2 h p.i.. Transmission scans (10 min) were performed before the dynamic and static image acquisition, respectively. The images were reconstructed with the Inveon Acquisition Workspace Software (Siemens) and OSEM 3D SP-MAP algorithm (16 subsets, 4 iterations, MAP Iteration: 18) using a 28 frame protocol (2x15s,8x30s,5x60s,5x120s,8x300s) for the dynamic scan and one frame for the static scan. Median root was applied prior correction and images were converted to SUV images.

To identify the subcutaneous tumor by fluorescence, optical imaging was performed after PET imaging. Mice were sacrificed and the skin was removed covering the subcutaneous xenograft tumors. Subsequently, the Odyssey CLx system (LI-COR Biosciences, excitation wavelength 800 nm) was used for locating the tumor by fluorescence. Tumor tissue was resected and another scan performed with the Odyssey CLx system to ensure complete tumor tissue removal.

Supplementary Figures

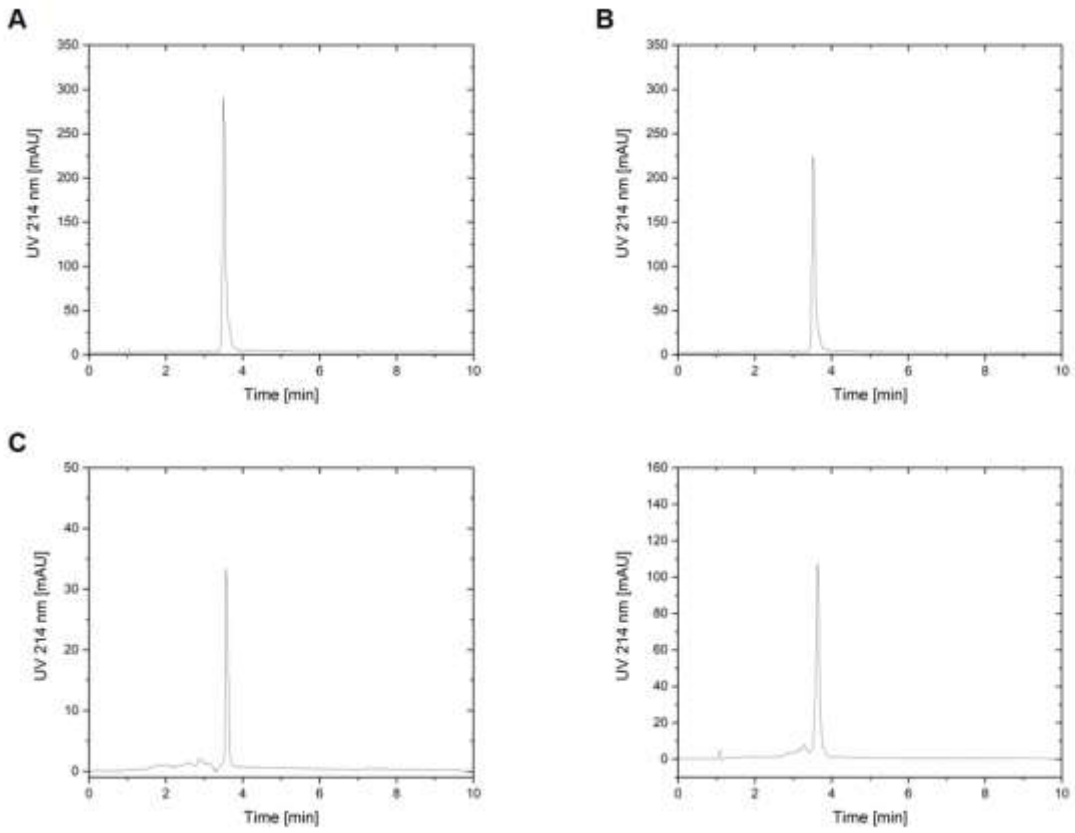

Supplemental Figure 3. Analytical HPLC of the compounds. Analytical reversed-phase HPLC of the final compounds was performed using a Chromolith RP-18e 100x4.6 mm column with a linear gradient (0.1% TFA in H_2O (A) to 100% B (0.1% TFA in CH_3CN)) in 10 min at 2 mL/min. UV trace at 214 nm is shown. (A) Glu-urea-Lys-$(HE)_1$-HBED-CC-IRDye800CW, (B) Glu-urea-Lys-$(WE)_1$-HBED-CC-IRDye800CW, (C) Glu-urea-Lys-$(HE)_3$-HBED-CC-IRDye800CW and (D) Glu-urea-Lys-HBED-CC-$(HE)_3$-IRDye800CW. Original data was plotted using OriginPro 2020 software.

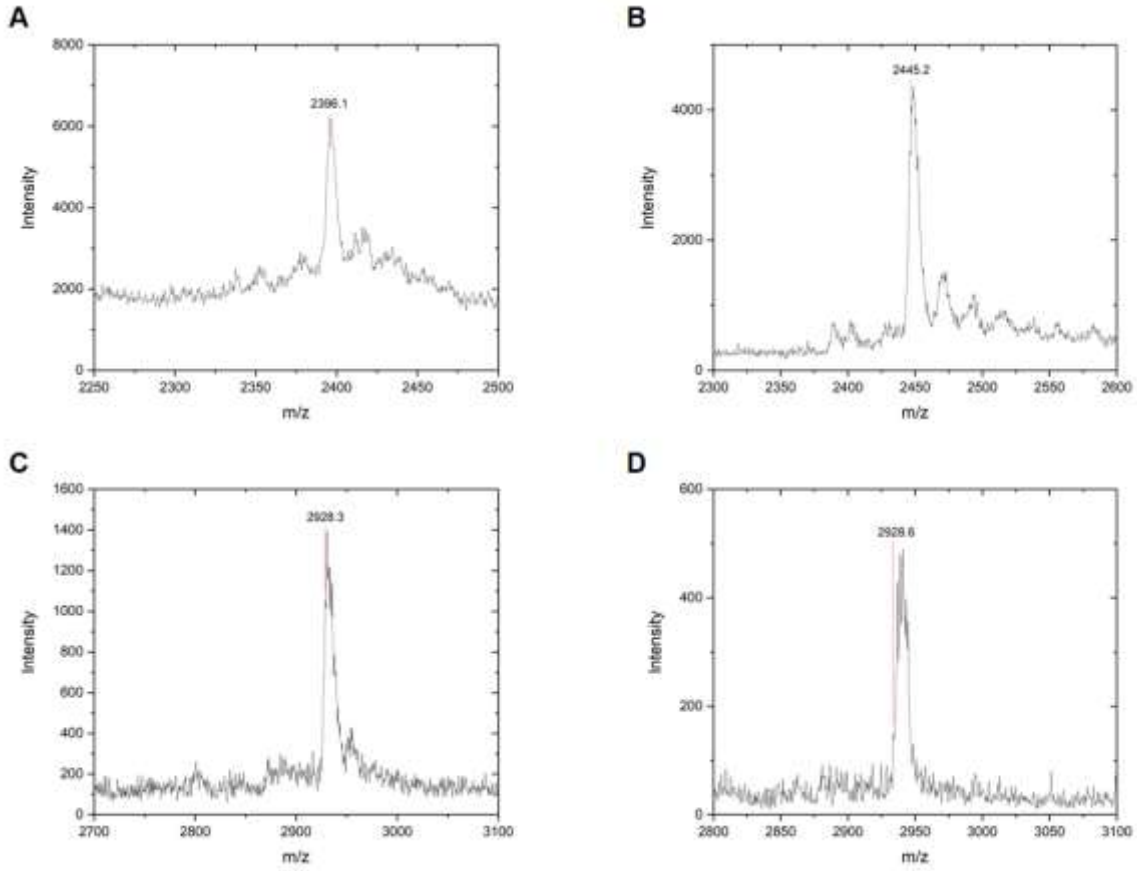

Supplemental Figure 4. MALDI spectra of the compounds. Mass spectrometry was performed with a MALDI-MS (Daltonics Microflex, Bruker Daltonics) and 2,5-dihydroxybenzoic acid as a matrix. (A) Glu-urea-Lys-$(HE)_1$-HBED-CC-IRDye800CW, (B) Glu-urea-Lys-$(WE)_1$-HBED-CC-IRDye800CW, (C) Glu-urea-Lys-$(HE)_3$-HBED-CC-IRDye800CW and (D) Glu-urea-Lys-HBED-CC-$(HE)_3$-IRDye800CW. Original data was plotted using OriginPro 2020 software.

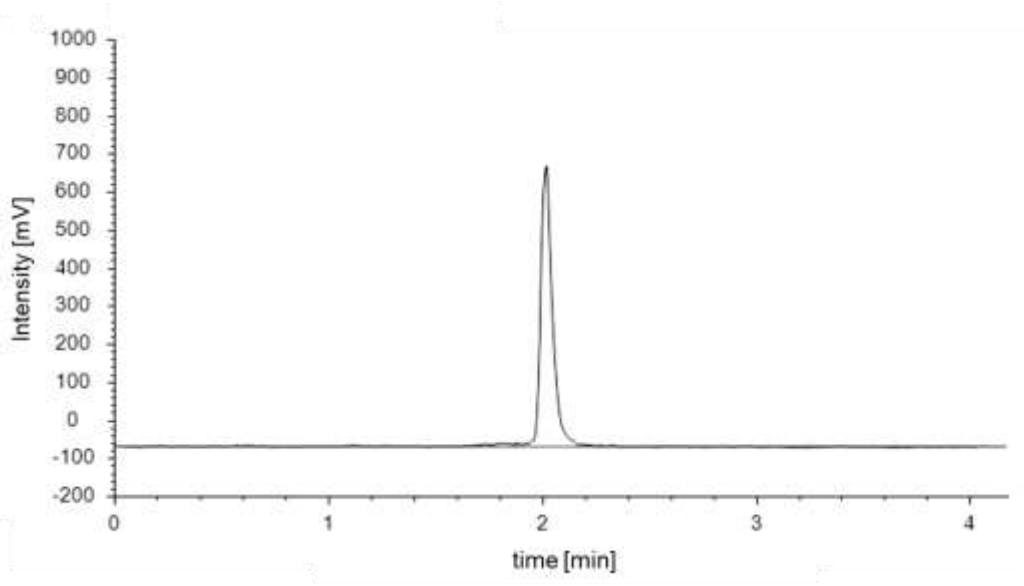

Supplemental Figure 5. Exemplary analytical radio-HPLC of ^{68}Ga-Glu-urea-Lys-(HE)$_3$-HBED-CC-IRDye800CW. Analytical reversed-phase HPLC of the ^{68}Ga-labeled compound was performed using a Chromolith RP-18e 100x4.6 mm column with a linear gradient (0.1% aqueous TFA (A) to 100% B (0.1% TFA in CH_3CN)) in 5 min at 4 mL/min. For radiodetection the system was equipped with a γ-detector.

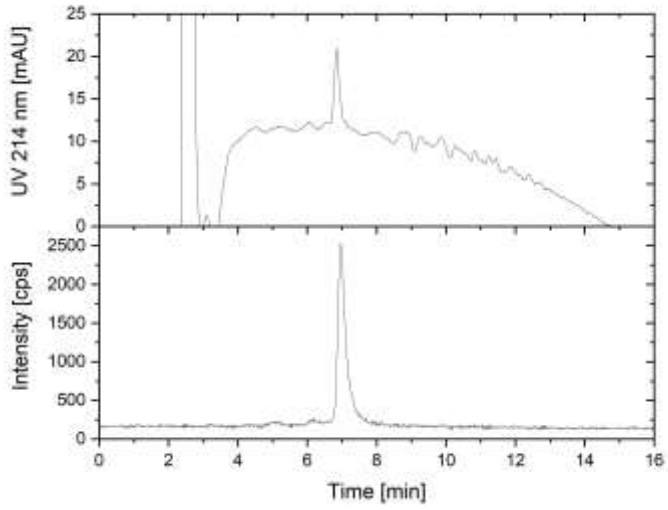

Supplemental Figure 6. HPLC of co-injected ^{68}Ga-Glu-urea-Lys-(HE)$_3$-HBED-CC-IRDye800CW and Glu-urea-Lys-(HE)$_3$-HBED-CC-IRDye800CW. Analytical reversed-phase HPLC of the ^{68}Ga-labeled compound co-injected with the non-radiolabeled precursor Glu-urea-Lys-(HE)$_3$-HBED-CC-IRDye800CW was performed using a EC 250/4.6 NUCLEOSIL 120-5 C 18 column (Machery-Nagel) with a linear gradient 85% 0.1% aqueous TFA (A) to 60% B (0.1% TFA in CH_3CN)) in 13 min at 1.5 mL/min. UV was measured at 214 nm and for radiodetection the system was equipped with a γ-detector. Original data was plotted using OriginPro 2020 software.

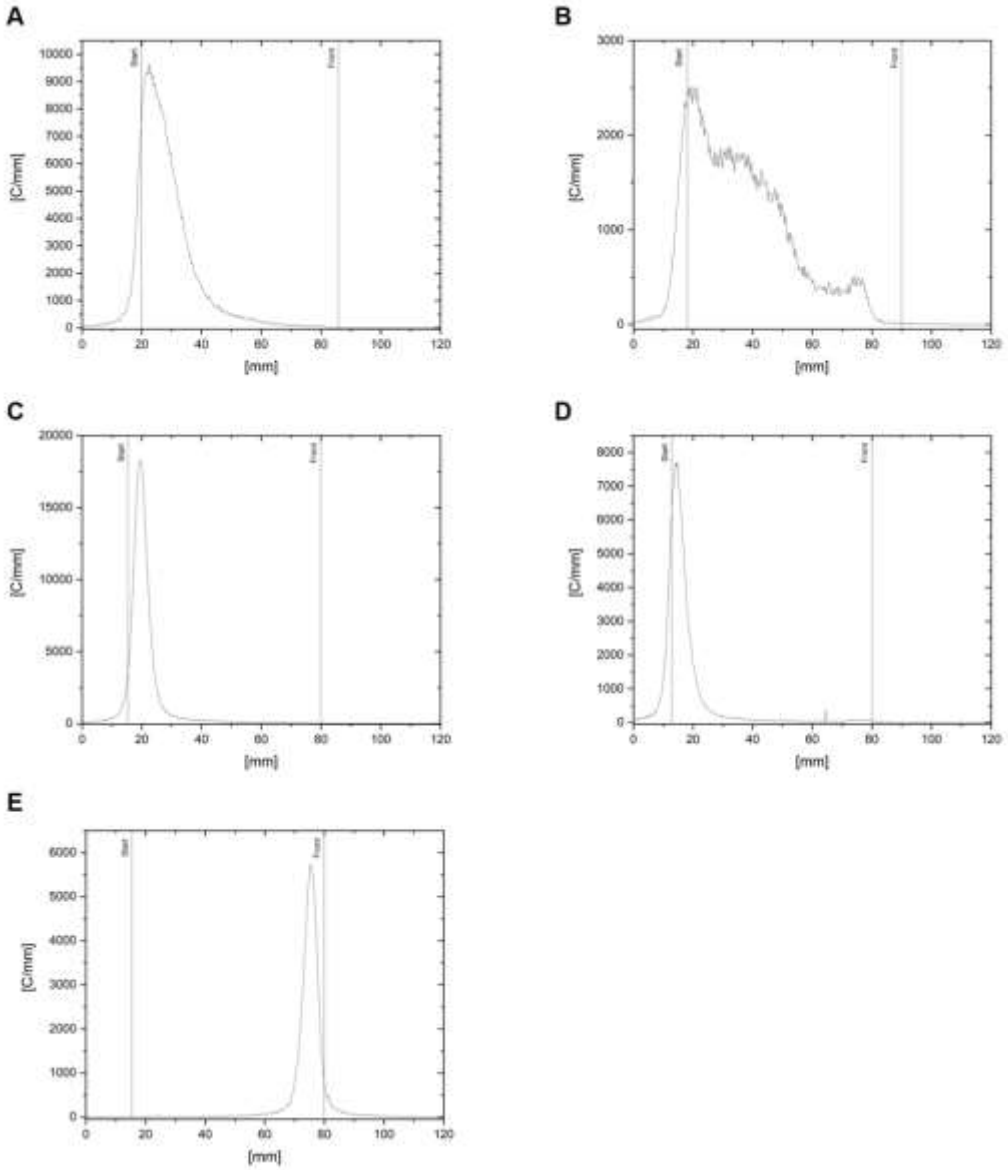

Supplemental Figure 7. Reversed-phase thin layer chromatography of ^{68}Ga-labeled compounds. RP-TLC (60 RP-18 F_{254S}) was performed with 0.1 M sodium citrate as mobile phase. (A) Glu-urea-Lys-$(HE)_1$-HBED-CC-IRDye800CW, (B) Glu-urea-Lys-$(WE)_1$-HBED-CC-IRDye800CW, (C) Glu-urea-Lys-$(HE)_3$-HBED-CC-IRDye800CW, (D) Glu-urea-Lys-HBED-CC-$(HE)_3$-IRDye800CW and (E) $^{68}GaCl_3$ as a control. Original data was plotted using OriginPro 2020 software.

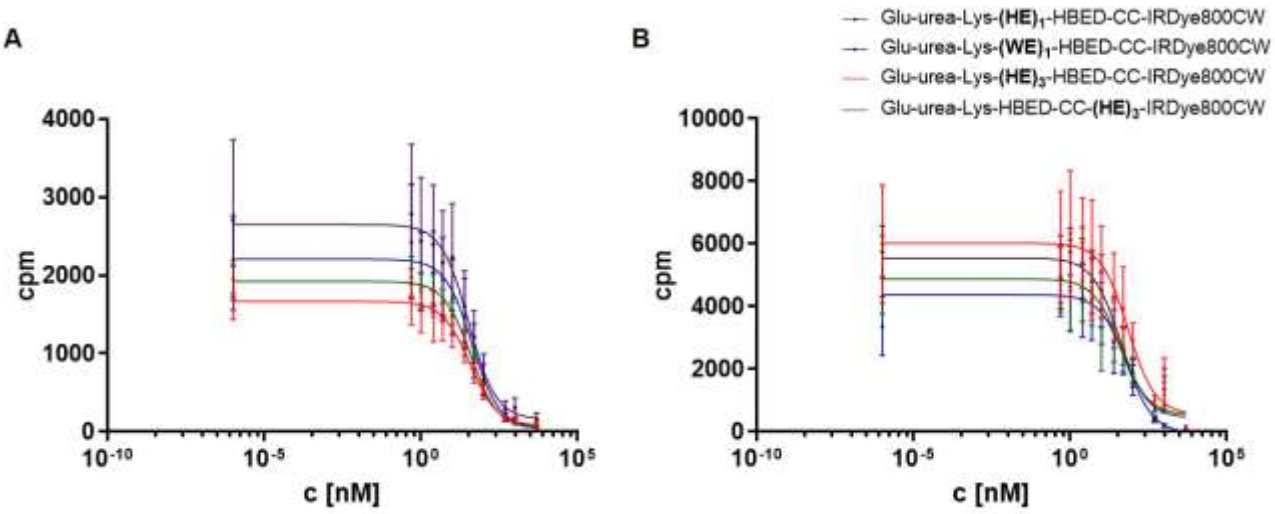

Supplemental Figure 8. Determination of binding affinity to PSMA. Binding affinity was determined on PSMA$^+$ LNCaP-cells with ^{68}Ga-PSMA-10 (K_d: 3.8 ± 1.8 nM (*1*), $c_{radioligand}$: 0.75 nM) as radioligand. IC_{50} curves of (A) free ligands and (B) $^{69/71}$Ga-labeled ligands were plotted with GraphPad Software. The 50% inhibitory concentration (IC50) values were calculated by fitting the data using a nonlinear regression algorithm (GraphPad Software).

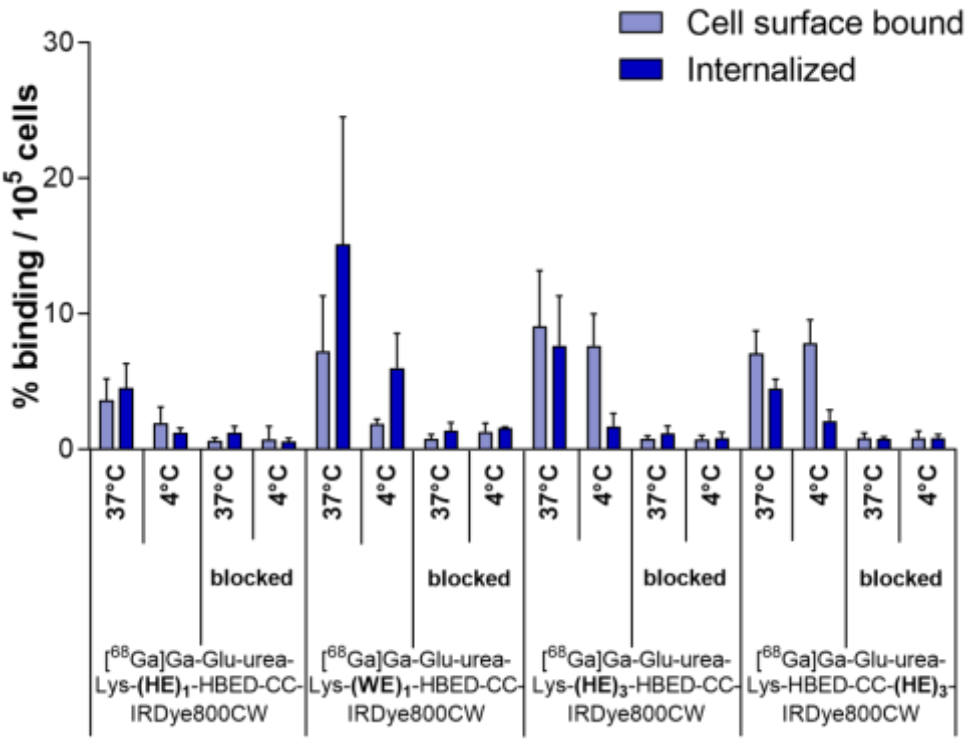

Supplemental Figure 9. Cell surface binding and internalization of ^{68}Ga-labeled compounds. Specificity of internalization was determined by blocking with 2-PMPA (500 µM) or incubating on ice at 4°C. Data are expressed in %binding/10^5 cells and represent mean ± standard deviation (n=3).

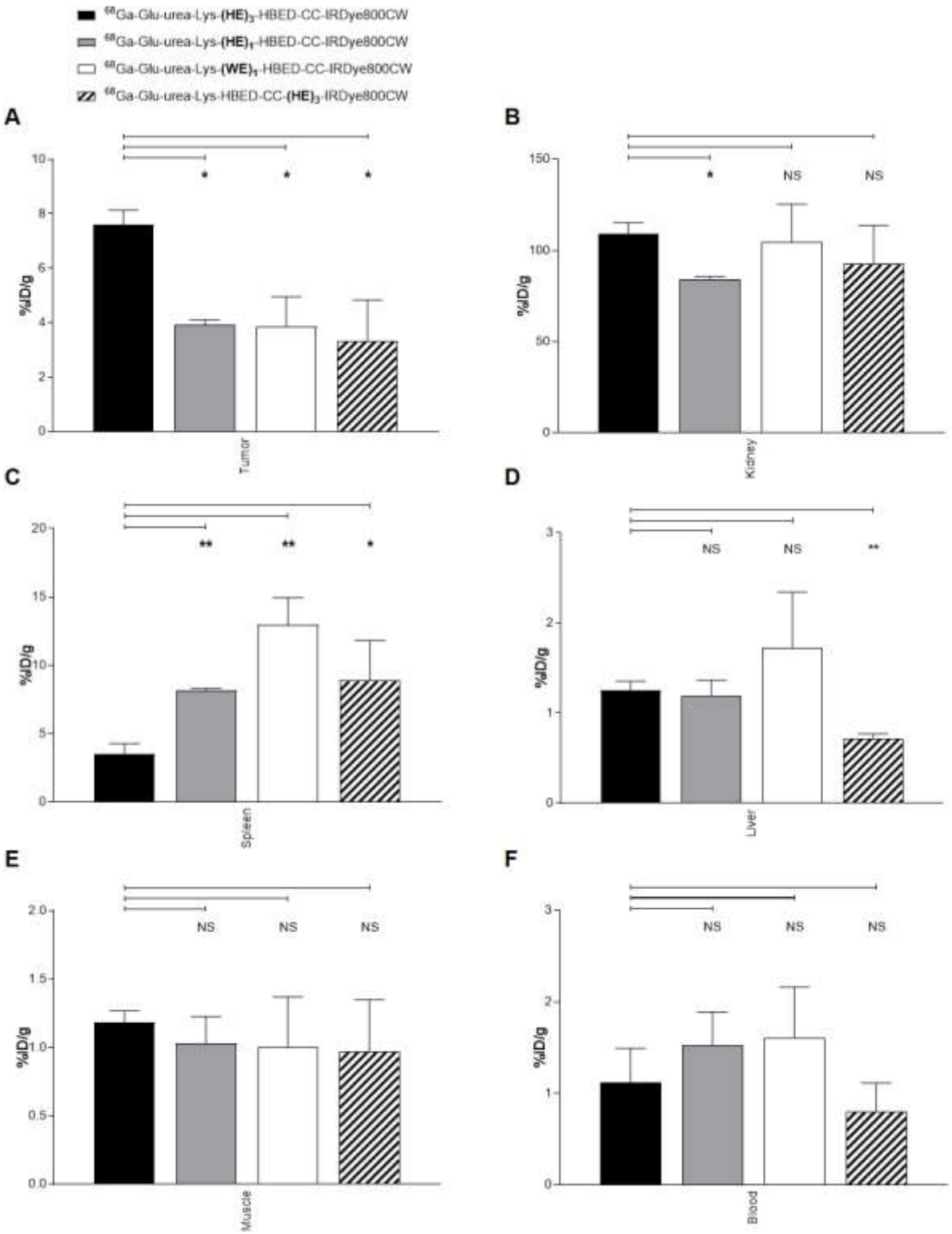

Supplemental Figure 10. Organ distribution of ^{68}Ga-labeled compounds. Organ distribution of 60 pmol ^{68}Ga-labeled compounds at 1 h p.i. with uptake in (A) PSMA^{+}-tumor (LNCaP), (B) kidney, (C) spleen, (D) liver, (E) muscle and (F) blood. Data are expressed as mean % ID/g tissue ± SD (n=3). Significant differences are presented with asterisks above the bars that are being compared (NS: not significant, *p<0.05, **p<0.01).

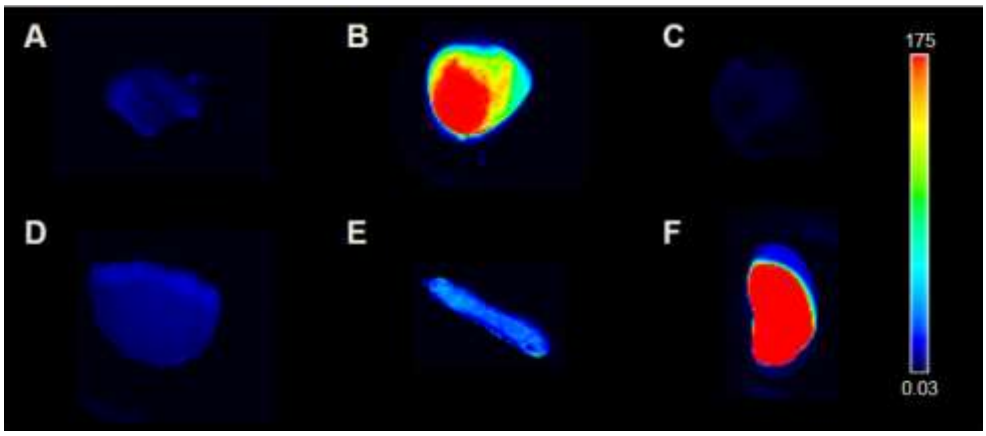

Supplemental Figure 11. Fluorescence imaging after organ distribution 1 h p.i.. Fluorescence imaging of organs dissected after injection of 0.5 nmol ^{68}Ga-labeled Glu-urea-Lys-(HE)$_3$-HBED-CC-IRDye800CW in LNCaP tumor-bearing BALB/c nu/nu mice 1 h p.i. (n=3, one representative image out of three is shown) acquired with the Odyssey CLx system (excitation wavelength 800 nm). Fluorescence intensity is presented in heat map colouring. (A) muscle, (B) PSMA$^+$-tumor (LNCaP), (C) blood (D) liver, (E) spleen, (F) kidney.

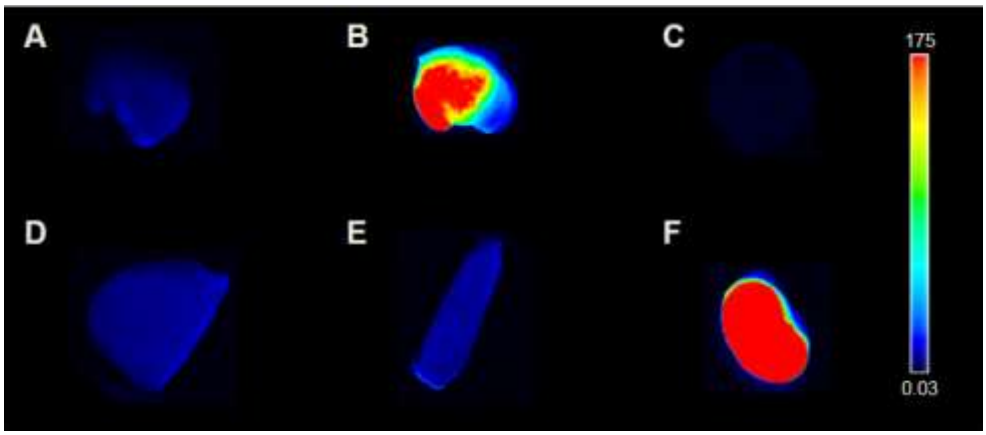

Supplemental Figure 12. Fluorescence imaging after organ distribution 2 h p.i.. Fluorescence imaging of organs dissected after injection of 0.5 nmol ^{68}Ga-labeled Glu-urea-Lys-(HE)$_3$-HBED-CC-IRDye800CW in LNCaP tumor-bearing BALB/c nu/nu mice 2 h p.i. (n=3, one representative image out of three is shown) acquired with the Odyssey CLx system (excitation wavelength 800 nm). Fluorescence intensity is presented in heat map colouring. (A) muscle, (B) PSMA$^+$-tumor (LNCaP), (C) blood (D) liver, (E) spleen, (F) kidney.

Supplementary Tables

Supplemental Table 1. Analytical data of the compounds.

Compound	Sum formula	m/z exact mass (calc.)	m/z*	Chemical yield [%]†	Lipophilicity log$D_{pH\ 7.4}$ *n-octanol/PBS*‡
Glu-urea-Lys-**(HE)$_1$**-HBED-CC-IRDye800CW	$C_{109}H_{144}N_{17}O_{36}S_4^+$	2394.9	2396.1	34	-3.15 ± 0.08
Glu-urea-Lys-**(WE)$_1$**-HBED-CC-IRDye800CW	$C_{114}H_{147}N_{16}O_{36}S_4^+$	2443.9	2445.2	12	-3.03 ± 0.05
Glu-urea-Lys-**(HE)$_3$**-HBED-CC-IRDye800CW	$C_{131}H_{172}N_{25}O_{44}S_4^+$	2927.1	2928.3	38	-1.65 ± 0.40
Glu-urea-Lys-HBED-CC-**(HE)$_3$**-IRDye800CW	$C_{131}H_{172}N_{25}O_{44}S_4^+$	2927.1	2928.6	17	-3.22 ± 0.08

* Mass spectrometry of non-labeled ligand detected as $[M+H]^+$, † Chemical yields refer to the fluorescent dye conjugation, ‡ Lipophilicity of ^{68}Ga-labeled ligand.

Supplemental Table 2. Chemical yields of the synthesis intermediates.

Intermediate	Chemical yield [%]
[Fe(HBED-CC-TFP_2)]	37
PEG_2-[Fe(HBED-CC-propargylamine)]	43
Glu-urea-Lys([Fe(HBED-CC-propargylamine)])	36
Glu-urea-Lys((HE)$_1$-CO$(CH_2)_4$-N_3)	66
Glu-urea-Lys((HE)$_3$-CO$(CH_2)_4$-N_3)	13
Glu-urea-Lys((WE)$_1$-CO$(CH_2)_4$-N_3)	58
PEG_2-(EH)$_3$-CO$(CH_2)_4$-N_3	35
Glu-urea-Lys((HE)$_1$-HBED-CC-PEG_2-NH_2)	15
Glu-urea-Lys((HE)$_3$-HBED-CC-PEG_2-NH_2)	23
Glu-urea-Lys((WE)$_1$-HBED-CC-PEG_2-NH_2)	16
Glu-urea-Lys([Fe(HBED-CC-(HE)$_3$-PEG_2-NH_2)])	13

Supplemental Table 3. Organ distribution of 0.06 nmol ^{68}Ga-labeled compounds in LNCaP-tumor bearing BALB/c nu/nu mice 1 h p.i.*.

	^{68}Ga-Glu-urea-Lys-**(HE)$_1$**-HBED-CC-IRDye800CW [%ID/g]	^{68}Ga-Glu-urea-Lys-**(WE)$_1$**-HBED-CC-IRDye800CW [%ID/g]	^{68}Ga-Glu-urea-Lys-**(HE)$_3$**-HBED-CC-IRDye800CW [%ID/g]	^{68}Ga-Glu-urea-Lys-HBED-CC-**(HE)$_3$**-IRDye800CW [%ID/g]
Blood	1.52 ± 0.64	1.61 ± 0.55	1.12 ± 0.64	0.80 ± 0.31
Heart	0.94 ± 0.14	1.49 ± 0.51	1.36 ± 0.37	0.57 ± 0.26
Lung	2.46 ± 0.46	2.57 ± 1.01	2.34 ± 0.37	1.78 ± 1.19
Spleen	8.17 ± 0.23	12.94 ± 2.00	3.47 ± 1.39	8.88 ± 2.93
Liver	1.19 ± 0.30	1.73 ± 0.61	1.25 ± 0.18	0.72 ± 0.05
Kidney	84.34 ± 2.13	104.58 ± 20.79	109.27 ± 10.33	92.54 ± 21.07
Muscle	1.03 ± 0.34	1.00 ± 0.37	1.18 ± 0.15	0.97 ± 0.38
Intestine	1.29 ± 0.36	0.96 ± 0.37	1.31 ± 0.00	0.65 ± 0.21
Brain	0.30 ± 0.10	0.15 ± 0.04	0.18 ± 0.02	0.18 ± 0.06
Tumor	3.92 ± 0.31	3.85 ± 1.10	7.59 ± 0.95	3.32 ± 1.51

***** Data are expressed as mean % ID/g tissue ± SD (n=3).

Supplemental Table 4. Tumor-to-organ ratios of 0.06 nmol ^{68}Ga-labeled compounds in LNCaP-tumor bearing BALB/c nu/nu mice 1 h p.i.*.

	^{68}Ga-Glu-urea-Lys-**(HE)$_1$**-HBED-CC-IRDye800CW	^{68}Ga-Glu-urea-Lys-**(WE)$_1$**-HBED-CC-IRDye800CW	^{68}Ga-Glu-urea-Lys-**(HE)$_3$**-HBED-CC-IRDye800CW	^{68}Ga-Glu-urea-Lys-HBED-CC-**(HE)$_3$**-IRDye800CW
Blood	3.01 ± 1.00	2.42 ± 0.21	8.81 ± 4.67	4.23 ± 1.02
Heart	4.39 ± 0.34	2.63 ± 0.34	5.72 ± 0.64	6.15 ± 1.56
Lung	1.69 ± 0.37	1.55 ± 0.23	3.27 ± 0.39	2.09 ± 0.46
Spleen	0.49 ± 0.03	0.30 ± 0.07	2.34 ± 0.47	0.38 ± 0.10
Liver	3.51 ± 0.86	2.26 ± 0.18	6.09 ± 0.13	4.61 ± 1.72
Kidney	0.05 ± 0.00	0.04 ± 0.01	0.07 ± 0.00	0.03 ± 0.01
Muscle	4.14 ± 1.32	3.96 ± 0.70	6.45 ± 0.09	3.51 ± 0.77
Intestine	3.35 ± 1.03	4.12 ± 0.38	5.80 ± 0.60	5.14 ± 1.15
Brain	14.97 ± 5.85	25.43 ± 2.13	42.66 ± 1.98	17.62 ± 2.14

***** Data are expressed as mean tumor-to-organ ratio ± SD (n=3).

Supplemental Table 5. Organ distribution of 0.06 nmol ^{68}Ga-labeled Glu-urea-Lys-(HE)$_3$-HBED-CC-IRDye800CW in PC-3-tumor bearing BALB/c nu/nu mice 1 h p.i.*.

	^{68}Ga-Glu-urea-Lys-**(HE)$_3$**-HBED-CC-IRDye800CW [%ID/g]	^{68}Ga-Glu-urea-Lys-**(HE)$_3$**-HBED-CC-IRDye800CW Tumor-to-Organ ratio
Blood	0.90 ± 0.21	0.58 ± 0.10
Heart	0.60 ± 0.21	0.88 ± 0.09
Lung	0.90 ± 0.36	0.60 ± 0.05
Spleen	1.30 ± 0.70	0.45 ± 0.08
Liver	0.53 ± 0.18	1.01 ± 0.04
Kidney	60.14 ± 32.59	0.01 ± 0.003
Muscle	0.21 ± 0.06	2.51 ± 0.20
Intestine	0.50 ± 0.23	1.11 ± 0.15
Brain	0.04 ± 0.01	14.33 ± 1.88
Tumor	0.53 ± 0.18	-

***** Data are expressed as mean % ID/g tissue ± SD (n=3) and Tumor-to-Organ ratios.

Supplemental Table 6. Organ distribution of 0.06 nmol ^{68}Ga-labeled Glu-urea-Lys-(HE)$_3$-HBED-CC-IRDye800CW in LNCaP-tumor bearing BALB/c nu/nu mice 2 h p.i.*.

	^{68}Ga-Glu-urea-Lys-**(HE)$_3$**-HBED-CC-IRDye800CW [%ID/g]	^{68}Ga-Glu-urea-Lys-**(HE)$_3$**-HBED-CC-IRDye800CW Tumor-to-Organ ratio
Blood	0.65 ± 0.01	4.73 ± 1.42
Heart	0.53 ± 0.08	5.84 ± 1.45
Lung	0.89 ± 0.05	3.43 ± 0.89
Spleen	0.76 ± 0.16	4.02 ± 0.70
Liver	0.76 ± 0.11	4.01 ± 0.77
Kidney	55.81 ± 9.76	0.06 ± 0.01
Muscle	0.47 ± 0.11	6.50 ± 0.95
Intestine	0.67 ± 0.17	4.66 ± 1.05
Brain	0.23 ± 0.15	14.83 ± 3.24
Tumor	3.10 ± 1.17	-

***** Data are expressed as mean % ID/g tissue ± SD (n=3) and Tumor-to-Organ ratios.

Supplemental Table 7. Organ distribution of 0.5 nmol ^{68}Ga-labeled Glu-urea-Lys-(HE)$_3$-HBED-CC-IRDye800CW in LNCaP-tumor bearing BALB/c nu/nu mice 1 h p.i.*.

	^{68}Ga-Glu-urea-Lys-**(HE)$_3$**-HBED-CC-IRDye800CW [%ID/g]	^{68}Ga-Glu-urea-Lys-**(HE)$_3$**-HBED-CC-IRDye800CW Tumor-to-Organ ratio
Blood	3.10 ± 1.40	6.89 ± 0.62
Heart	2.64 ± 0.59	7.87 ± 0.60
Lung	4.27 ± 1.02	4.96 ± 0.95
Spleen	6.90 ± 3.21	3.15 ± 0.62
Liver	2.43 ± 0.62	8.55 ± 0.61
Kidney	229.08 ± 53.38	0.09 ± 0.01
Muscle	1.17 ± 0.13	17.84 ± 2.26
Intestine	2.66 ± 0.89	7.89 ± 0.32
Brain	0.15 ± 0.06	144.46 ± 27.52
Tumor	20.98 ± 6.54	-

***** Data are expressed as mean % ID/g tissue ± SD (n=3) and Tumor-to-Organ ratios.

Supplemental Table 8. Organ distribution of 0.5 nmol ^{68}Ga-labeled Glu-urea-Lys-(HE)$_3$-HBED-CC-IRDye800CW in LNCaP-tumor bearing BALB/c nu/nu mice 2 h p.i.*.

	^{68}Ga-Glu-urea-Lys-**(HE)$_3$**-HBED-CC-IRDye800CW [%ID/g]	^{68}Ga-Glu-urea-Lys-**(HE)$_3$**-HBED-CC-IRDye800CW Tumor-to-Organ ratio
Blood	1.91 ± 0.84	6.56 ± 0.98
Heart	1.34 ± 0.73	9.45 ± 0.72
Lung	2.07 ± 0.89	6.04 ± 0.94
Spleen	2.26 ± 1.16	5.57 ± 0.50
Liver	1.62 ± 0.86	7.79 ± 0.75
Kidney	176.10 ± 97.86	0.07 ± 0.01
Muscle	0.56 ± 0.37	23.08 ± 0.81
Intestine	1.30 ± 0.56	9.91 ± 2.18
Brain	0.09 ± 0.05	138.96 ± 25.36
Tumor	12.90 ± 8.46	-

***** Data are expressed as mean % ID/g tissue ± SD (n=3) and Tumor-to-Organ ratios.

References

1. Schafer M, Bauder-Wust U, Leotta K, et al. A dimerized urea-based inhibitor of the prostate-specific membrane antigen for 68Ga-PET imaging of prostate cancer. *EJNMMI Res.* 2012;2:23.

2. Eder M, Wangler B, Knackmuss S, et al. Tetrafluorophenolate of HBED-CC: a versatile conjugation agent for 68Ga-labeled small recombinant antibodies. *Eur J Nucl Med Mol Imaging.* 2008;35:1878-1886.